Bandwidth and crosstalk considerations in a spatio-temporally modulated polarimeter

Israel J. Vaughn[a], Oscar G. Rodríguez-Herrera[b], Mohan Xu[a], J. Scott Tyo[a,c]

[a]College of Optical Sciences, University of Arizona, Tucson, USA;
[b]Centro de Ciencias Aplicadas y Desarrollo Tecnológico,Universidad Nacional Autónoma de México, Cd. Universitaria, México
[c]University of New South Wales @ ADFA, Canberra, ACT, Australia

ABSTRACT

Recently we designed and built a portable imaging polarimeter for remote sensing applications.[1] Polarimetric imaging operators are a class of linear systems operators in the Mueller matrix reconstruction space, resulting in a set of measurement channels.[2] The nature of remote sensing requires channel crosstalk to be minimized for either general Mueller matrix reconstruction or task specific polarimetric remote sensing. We illustrate crosstalk issues for a spatio-temporally modulated Mueller matrix reconstruction operator, and show how to minimize channel crosstalk by maximizing bandwidth between channels. Specifically channel cancellation allows increases in channel bandwidth. We also address the impact that systematic deviations from the ideal operators and i.i.d. noise have on the system channel structure.

Keywords: polarimetry, modulated polarimetry, linear systems, active polarimetry, Mueller matrix, aliasing, crosstalk

1. INTRODUCTION

Channeled Mueller matrix polarimeters and the concept of using these channels was first introduced by Azzam.[3] Azzam published a very specific case, 1) a specific temporal framework was analyzed, 2) an implicit assumption about the object was made, *the object had no temporal bandwidth*, i.e., the object was stationary in time. Oka, Sabatke, Derniak, Kudenov, and Hagen then demonstrated both spectrally channeled and spatially (over spectrum) channeled systems,[4–10] mostly Stokes polarimeters. Dubreuil *et al*[11] then presented a spectrally channeled Mueller matrix polarimeter, which of course is non-imaging since the focal plane array is used to resolve the spectrum. LaCasse, Chipman, Tyo, and LeMaster and Hirakawa[12–14] then described micropolarizer array partial Stokes polarimeters as channeled systems, and LaCasse *et al* presented a spatio-temporally modulated hybrid channeled Stokes system,[15] and subsequently both Myhre *et al*[16] and Zhao *et al*[17] presented spatially modulated full Stokes polarimeters. Finally Alenin and Tyo[2] formalized a general framework which describes channeled polarimeters almost completely, both Mueller and Stokes.

Prior to the work by LaCasse *et al*,[12,13,15] bandwidth in channeled polarimetric systems had not been addressed, or only addressed as a consequence of instrumental "error." Additionally, prior to Alenin and Tyo[2] channeled systems were designed in an *ad-hoc* manner. In this communication we address bandwidth using the *systematic* design tools introduced by Alenin and Tyo[2] for a hybrid spatio-temporally modulated channeled active polarimetric system.

Send correspondence to IJV or JST
IJV: israel.vaughn@gmail.com
JST: S.Tyo@adfa.edu.au

2. FORMALISM AND CHANNELS

Note that this section originally appeared in our other publication in this conference proceeding[1] and is derived/adapted from that section to address the topic of this communication for ease of reference. Portions may be reproduced verbatim, however quotes will not be used.

We use the Mueller-Stokes mathematical formalism here, as it is most commonly used in instrumental polarization and polarimeter design. This analysis is, however, agnostic to the formalism used, a coherence formalism[18] with periodic modulators could also be used and would have similar results. In the next sections, it should be kept in mind that modulations are done in some physical domain, they are periodic, i.e., a superposition of sinusoidal functions, and the "channels" are the resultant δ-functions which ensue from the Fourier transform of the sinusoidal modulations.

2.1 Modulated Mueller formalism

The Stokes parameters are described by

$$\boldsymbol{s} = \begin{bmatrix} s_0 \\ s_1 \\ s_2 \\ s_3 \end{bmatrix} \propto \begin{bmatrix} \langle |E_x|^2 \rangle + \langle |E_y|^2 \rangle \\ \langle |E_x|^2 \rangle - \langle |E_y|^2 \rangle \\ 2\,\mathrm{Re}\,\langle E_x E_y^* \rangle \\ 2\,\mathrm{Im}\,\langle E_x E_y^* \rangle \end{bmatrix} = \begin{bmatrix} \\ \\ \\ \\ \end{bmatrix}, \text{ where } s_0 > 0,\ \ s_0^2 \geq s_1^2 + s_2^2 + s_3^2 \tag{1}$$

where $\langle \cdot \rangle$ denotes the time average, s_0 is proportional to the total irradiance, s_1 is proportional to the prevalence of horizontal (0°) over vertical (90°) polarization, s_2 is proportional to the prevalence of +45° over −45° polarization, and s_3 is proportional to the prevalence of right circular over left circular polarization.[19] Because optical sensors measure a quantity proportional to the time averaged Poynting vector, the phase information is lost, and only the incoherent time averaged polarization information can be obtained.[18,19]

For materials which can be described via linear optical interactions, we can use the Mueller-Stokes formalism. A Mueller matrix, $\boldsymbol{M}$, is a matrix which linear transforms one set of Stokes parameters, $\boldsymbol{s}_{\text{in}}$, into another set of Stokes parameters, $\boldsymbol{s}_{\text{out}}$:

$$\boldsymbol{s}_{\text{out}} = \boldsymbol{M} \cdot \boldsymbol{s}_{\text{in}} \tag{2}$$

Notice that $\boldsymbol{M} \in \mathbb{R}^{4\times 4}$ but not every 4×4 real valued matrix is a Mueller matrix due to the constraints in Eqn.1, see Gil[20] for details.

With an active, or Mueller matrix, polarimeteric instrument, we must modulate in irradiance to infer the Mueller matrix of an object, $\boldsymbol{M}(\boldsymbol{x})$, where $\boldsymbol{x} = \begin{bmatrix} x & y & z & t & \sigma \end{bmatrix}^T$. We can then rewrite Eqn. 2 to have Mueller matrices and Stokes parameters be functions of space, time, and wavelength or wavenumber. Eqn.2 then becomes

$$\begin{bmatrix} s_{0,\text{out}}(\boldsymbol{x}) \\ s_{1,\text{out}}(\boldsymbol{x}) \\ s_{2,\text{out}}(\boldsymbol{x}) \\ s_{3,\text{out}}(\boldsymbol{x}) \end{bmatrix} = \begin{bmatrix} m_{00}(\boldsymbol{x}) & m_{01}(\boldsymbol{x}) & m_{02}(\boldsymbol{x}) & m_{03}(\boldsymbol{x}) \\ m_{10}(\boldsymbol{x}) & m_{11}(\boldsymbol{x}) & m_{12}(\boldsymbol{x}) & m_{13}(\boldsymbol{x}) \\ m_{20}(\boldsymbol{x}) & m_{21}(\boldsymbol{x}) & m_{22}(\boldsymbol{x}) & m_{23}(\boldsymbol{x}) \\ m_{30}(\boldsymbol{x}) & m_{31}(\boldsymbol{x}) & m_{32}(\boldsymbol{x}) & m_{33}(\boldsymbol{x}) \end{bmatrix} \cdot \begin{bmatrix} s_{0,\text{in}} \\ s_{1,\text{in}} \\ s_{2,\text{in}} \\ s_{3,\text{in}} \end{bmatrix} \tag{3}$$

where for simplicity we fix $\boldsymbol{s}_{\text{in}}$. Our detector then measures a quantity proportional to $s_{0,\text{out}}(\boldsymbol{x})$. For a Mueller matrix measuring instrument, we have an unknown object Mueller matrix, $\boldsymbol{M}_{\text{obj}}(\boldsymbol{x})$, and we write down the instrument equation which modulates Stokes parameters:[21]

$$\begin{aligned} \boldsymbol{s}_{\text{out}}(\boldsymbol{x}) &= \boldsymbol{A}(\boldsymbol{x}) \cdot \boldsymbol{M}_{\text{obj}}(\boldsymbol{x}) \cdot \boldsymbol{G}(\boldsymbol{x}) \cdot \boldsymbol{s}_{\text{in}} \qquad (4) \\ &= \boldsymbol{A}(\boldsymbol{x}) \cdot \boldsymbol{M}_{\text{obj}}(\boldsymbol{x}) \cdot \boldsymbol{s}_{\boldsymbol{G}}(\boldsymbol{x}) \qquad (5) \end{aligned}$$

where $\boldsymbol{G}(\boldsymbol{x}), \boldsymbol{A}(\boldsymbol{x})$ are the generator and analyzer Mueller matrices respectively, known and modulated via the physical instrument. The generator modulation can then be thought of as only a Stokes parameter modulation, $\boldsymbol{s}_{\boldsymbol{G}}(\boldsymbol{x})$.

2.2 Channels

Eqn.5 can be expanded to obtain a linear equation[19] for $s_{0,\text{out}}(\boldsymbol{x})$.

$$\boxed{s_{0,\text{out}}(\boldsymbol{x}) = \sum_{i=0}^{3}\sum_{j=0}^{3} a_{0i}(\boldsymbol{x}) s_j(\boldsymbol{x}) m_{ij}(\boldsymbol{x})} \tag{6}$$

where $a_{0i}(\boldsymbol{x})$ are the elements of the first row of $\boldsymbol{A}(\boldsymbol{x})$, $s_j(\boldsymbol{x})$ are elements of $\boldsymbol{s_G}(\boldsymbol{x})$, and $m_{ij}(\boldsymbol{x})$ are elements of $\boldsymbol{M}_{\text{obj}}(\boldsymbol{x})$. We can then take the Fourier transform of $s_{0,\text{out}}(\boldsymbol{x})$ to obtain

$$\boxed{S_{0,\text{out}}(\boldsymbol{\rho}) = \sum_{i=0}^{3}\sum_{j=0}^{3} A_{0i}(\boldsymbol{\rho}) * S_j(\boldsymbol{\rho}) * M_{ij}(\boldsymbol{\rho})} \tag{7}$$

Where $\boldsymbol{x} \to \boldsymbol{\rho}$ in the Fourier transform, $*$ denotes convolution, and the shift to capital letters indicates a function has been Fourier transformed. If $a_{0i}(\boldsymbol{x})$ and $s_j(\boldsymbol{x})$ are superpositions of sinusoidal functions, then $A_{0i}(\boldsymbol{\rho}) * S_j(\boldsymbol{\rho})$ is a set of δ-functions, and each $M_{ij}(\boldsymbol{\rho})$ is then convolved with each δ-function in the set. The complete set of δ-functions for the system

$$\sum_{i=0}^{3}\sum_{j=0}^{3} A_{0i}(\boldsymbol{\rho}) * S_j(\boldsymbol{\rho}) \tag{8}$$

are defined as the *channels* of the system, or the system's *channel structure*.[2]

2.3 System equation

All examples in this communication will assume a quad-retarder + micropolarizer array Mueller matrix polarimeter system. This results in a spatio-temporally modulated system channel structure. The details of the design and an actual instrument implementation are in Vaughn *et al*[1] and the system equation is reproduced below:

$$\boldsymbol{s}_{\text{out}} = \boldsymbol{P}(x,y) \cdot \boldsymbol{R}(\nu_4, \epsilon_4, \delta_4) \cdot \boldsymbol{R}(\nu_3, \epsilon_3, \delta_3) \cdot \boldsymbol{M}_{\text{obj}}(x,y,t) \cdot \boldsymbol{R}(\nu_2, \epsilon_2, \delta_2) \cdot \boldsymbol{R}(\nu_1, \epsilon_1, \delta_1)\boldsymbol{s}_{\text{in}} \tag{9}$$

where

$$\boldsymbol{P}(x,y) = \text{micropolarizer array Mueller matrix} \tag{10}$$
$$\boldsymbol{R}(\nu_j, \epsilon_j, \delta_j) = \text{retarder Mueller matrix} \tag{11}$$
$$\nu_j = \text{retarder frequency in } 2\pi\frac{radians}{s} \tag{12}$$
$$\epsilon_j = \text{retarder start position in } 2\pi\, radians \tag{13}$$
$$\delta_j = \text{retarder retardance in } radians \tag{14}$$
$$\boldsymbol{M}_{\text{obj}}(x,y,t) = \text{Mueller matrix of the object} \tag{15}$$

Where of course only the final irradiance value, proportional to the $s_{0,\text{out}}(\boldsymbol{x})$ element of $\boldsymbol{s}_{\text{out}}(\boldsymbol{x})$ is sampled. The channels are encoded in $s_{0,\text{out}}(\boldsymbol{x})$.

3. CHANNEL DESIGN

Designing polarimetric instruments using a channeled framework is somewhat new in the field, especially for instruments which are not spectrally modulated. Spectral instrument designers have, however, utilized channel design in an *iterative* way, tweaking the system designs and then observing the channels which result, then again tweaking the system design. Here, we specify constraints and needs, and then optimize the system *directly in the channel space* for some cost function dependent on those specifications. This design paradigm allows for faster and (sometimes) conceptually simpler system configuration.

We will only address spatio-temporally modulated systems here, and we assume modulations are of the type

$$f(x, y, t) = h(x, y) \cdot g(t), \tag{16}$$

i.e., that any modulation is mathematically separable between time and space. Non-separable modulations can be constructed (envision a rotating focal plane array with a micropolarizer, or a spatial light modulator modulating in time and spatially), but we will address these in a future publication. A separable system only allows for bandwidth improvements from channel cancellations or combinations, while a non-separable system may allow for improvements from rotations of the channel structure, however the latter remains an open question. We emphasize once again that the channels are δ-functions in the Fourier domain which result from *sinusoidal modulations of irradiance in the physical domain*, i.e. space, time, wavelength, etc.

3.1 Notation

Visualization of channel structures can be accomplished by graphing the sets of channels, or δ-functions over the Fourier domain dual to the physical modulation domain. Another systematic way of graphing the modulations is the *frequency phase matrix* (FPM), introduced by Alenin and Tyo,[2] which is a book keeping method for the channel splitting behavior, the signs, and real and imaginary components of the δ-functions. In this communication we will graph the channels as they actually appear in the channel space to reinforce intuition and understanding.

Table 1: Notation for channels.

	positive	negative
real	△	▽
imag.	▷	◁

A δ-function can be characterized by its position, and its complex magnitude. Table 1 outlines the graphical notation that we will use, the blue triangles represent the real part of the magnitude, red triangles represent the imaginary part of the magnitude, the directions that the triangles point represent whether the magnitude is positive or negative, and size of each triangle represents the absolute value of the real part or the imaginary part. Note that we will only show the channels for a single Mueller matrix element for each visualization, with the channels for all other Mueller matrices represented by light gray-blue circles. Keep in mind that many channels, for each Mueller matrix element, end up being added together at the locations shown. Again, the relationship between the channels of different Mueller matrices is *additive*. An example of the channel structure for a spatio-temporally modulated system for m_{23} is shown in Fig.1.

Some of the examples presented here will be normalized to a temporal frequency range of $[-1, 1]$, this is because for instrument design only the relative frequencies are important, we are always limited by some maximum sampling rate in practice, so relative bandwidth with respect to a maximum absolute frequency of 1 is what must be optimized for. Due to the assumption of separable modulation functions for space and time and Mueller matrix physicality conditions, channels are fixed to travel along constrained paths in the Fourier domain.

3.2 Optimization

Once some spatio-temporal modulation scheme is selected, and the free parameters of that scheme are known, an optimization over the parameters for some specific cost function can be carried out. Alenin and Tyo[2,22] have used cost functions which optimize the spectral channel structure for noise performance, but other cost functions may be used. In this communication, we jointly optimize for bandwidth and noise using the following cost function:

$$\mathcal{O}(\boldsymbol{p}) = \frac{[CN(\boldsymbol{p})]^n}{\mathrm{dist}(\boldsymbol{p})}. \tag{17}$$

where $\boldsymbol{p}$ is a vector of free parameters which control the channel structure, the $\mathrm{dist}(\boldsymbol{p})$ function quantifies the distance between channels, i.e., bandwidth, $CN(\boldsymbol{p})$ is the condition number of the "mixing matrix" $\boldsymbol{Q}$ (details about $\boldsymbol{Q}$ are in Alenin and Tyo[2]), and $n \in \mathbb{R}^+$ is a weighting parameter for condition number corresponding to noise optimization. This is valid since $CN \geq 1$ by definition. The optimization then minimizes $\mathcal{O}(\boldsymbol{p})$ over $\boldsymbol{p}$. Note that as we increase n, the optimization tends to favor noise performance over bandwidth. A system conditioning

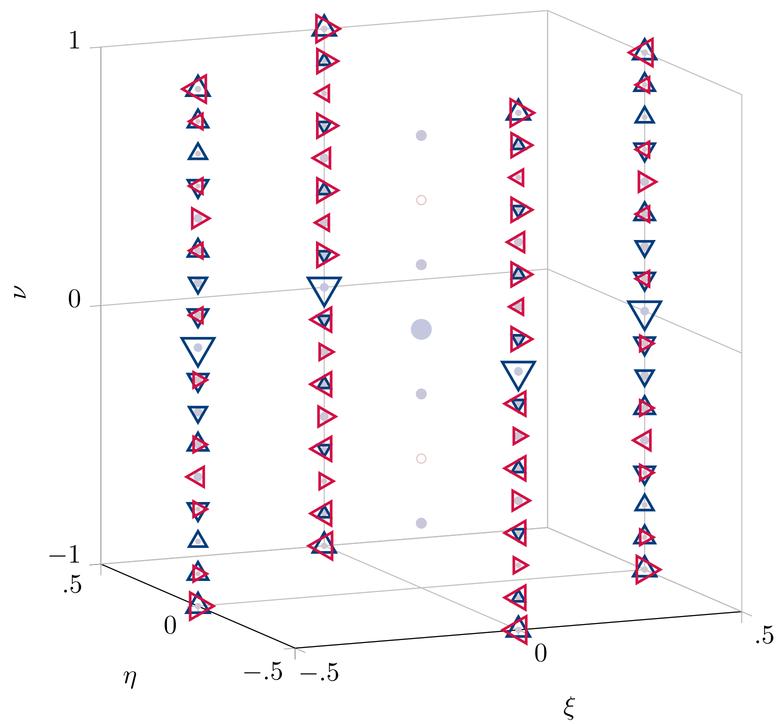

Figure 1: Example of a spatio-temporal channel structure with δ-functions specific to m_{23}. The maximum bandwidth corresponds to the minimum distance between two adjacent channels, taken over all possible adjacent channel pairs.

metric must be included in the cost function to ensure reconstructablility of the full Mueller matrix, i.e., higher bandwidths can be found which result in some partial Mueller matrix polarimeter (pMMP) reconstruction, but the system conditioning would be infinite for the full Mueller matrix reconstruction. This fact has utility for pMMP designs, but will not be addressed here.

4. BANDWIDTH

The treatment of bandwidth for channeled systems is mature and well known in information and communications theory.[23–25] The difficulties of using a channeled systems framework for polarimetric instruments are primarily 1) constructing channels in 2 or more dimensions (many systems in communications theory are 1 dimensional), 2) addressing physicality constraints in an analytical way, and 3) addressing the complicated channel mixing behavior that is inherent to polarimetric instruments. 3) has mostly been addressed by Alenin and Tyo.[2] 2) is a complicated subject and we will not delve into details here, but we emphasize again that these constraints must be enforced when optimizing for some cost function.

We will discuss a spatio-temporal system, with modulation in the domain

$$\boldsymbol{x} = \begin{bmatrix} x \\ y \\ t \end{bmatrix} \tag{18}$$

and examples will be from a quad-retarder + micropolarizer array system.[1] First we will briefly review convolution. Given some unknown quantity, $m(t)$, this quantity can be modulated with a sinusoidal function. Without

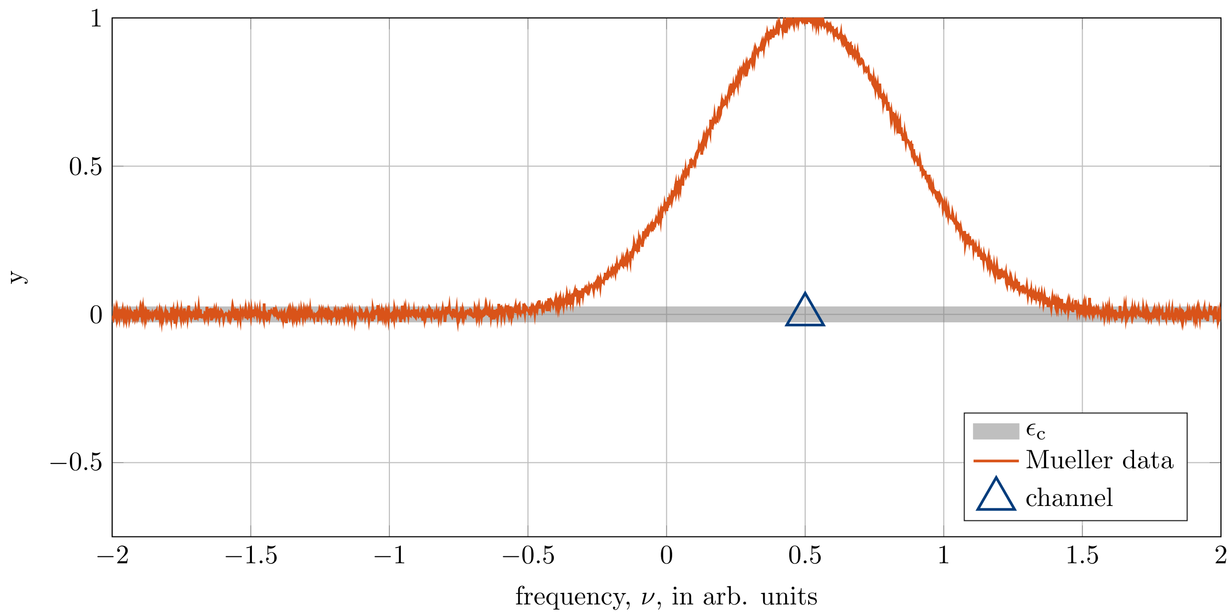

Figure 2: An example of convolution of data with a channel. The gray band represents the range of ϵ_c, resulting in data being outside of the ϵ_c range for $-0.5 < \nu < 1.5$. This implies a bandwidth of 2 arb. units for the Mueller data.

loss of generality, we choose cosine here:

$$f(t) = \cos 2\pi\nu_0 t \cdot m(t) \tag{19}$$
$$\implies \mathcal{F}\left\{f(t)\right\}_{t\to\nu} = \mathcal{F}\left\{\cos 2\pi\nu_0 t \cdot m(t)\right\}_{t\to\nu} \tag{20}$$
$$\implies F(\nu) = \mathcal{F}\left\{\cos 2\pi\nu_0 t\right\}_{t\to\nu} * \mathcal{F}\left\{m(t)\right\}_{t\to\nu} \tag{21}$$
$$\implies F(\nu) = \frac{1}{2}\left[\delta(\nu-\nu_0) + \delta(\nu+\nu_0)\right] * M(\nu) \tag{22}$$
$$\implies F(\nu) = \frac{M(\nu-\nu_0)}{2} + \frac{M(\nu+\nu_0)}{2} \tag{23}$$

where $\mathcal{F}\left\{\cdot\right\}$ is the Fourier transform, $*$ is convolution, and $\delta(\nu)$ is the Dirac delta function. The last line is due to property of convolution with delta functions. This gives us some tools for conceptual descriptions for the forward problem and hence the bandwidth. There will exist a set of channels (δ-functions) for each Mueller matrix element $M_{ij}(\boldsymbol{\rho})$ in the Fourier domain. For each channel in that set, $M_{ij}(\boldsymbol{\rho})$ will be copied at that channel's location with $M_{ij}(\mathbf{0})$ being located precisely where the delta function is located. We can then define the bandwidth of M_{ij} for some threshold $\epsilon_c \geq 0$ as the values of $\boldsymbol{\rho}$ where $|M_{ij}(\boldsymbol{\rho})| > \epsilon_c$. Fig.2 clarifies these concepts.

The polarimetric system channel structure contains constraints on bandwidth because there is a finite distance between channels as shown in Fig.1. The channel structure determines the bandwidth available for reconstruction. When the bandwidth of the data becomes greater than the available bandwidth, then channel crosstalk occurs.

5. CROSSTALK

Crosstalk is similar to aliasing, but not the same phenomenon. Crosstalk is the result of limited channel bandwidth, and information (convolutions of data) in the channel exceeding the bandwidth of that channel and ”spilling or bleeding” over to an adjacent channel. Crosstalk is a result of the choice of channel structure, as opposed to the sampling rate (aliasing), even a continuously sampled channeled (unaliased) system can have crosstalk. An example of crosstalk is shown in Fig.3.

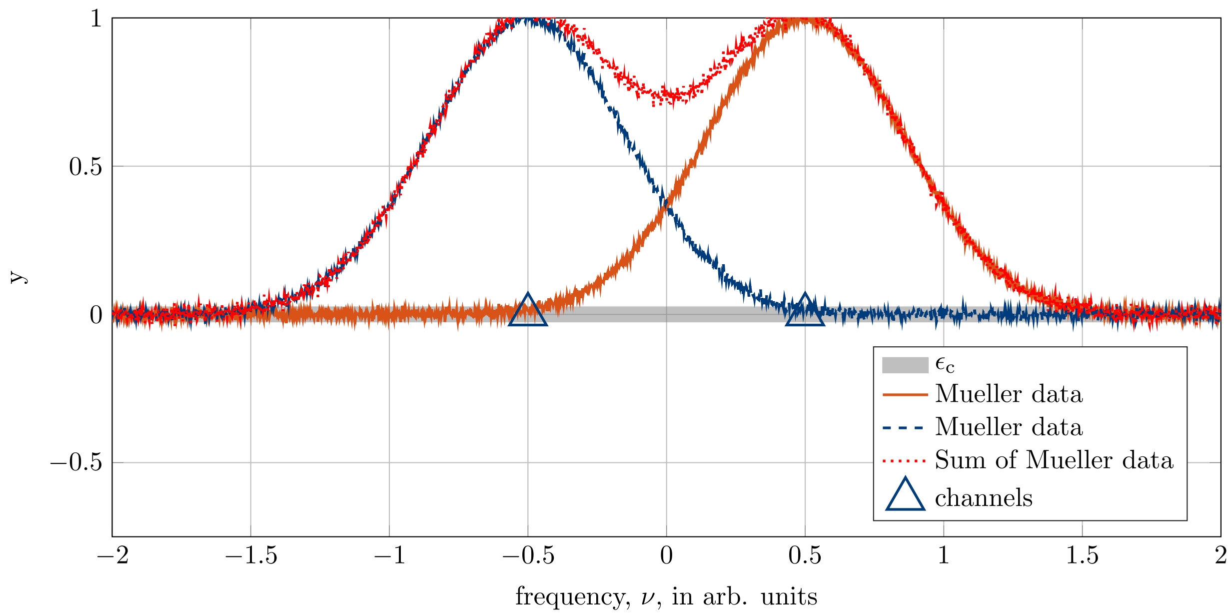

Figure 3: An example of channel crosstalk. Mueller data is placed at two channels, with the distance (bandwidth) between them less than the bandwidth of the Mueller data. When added, the Mueller data from different channels adds together, leaving no remedy to differentiate data between channels in the region of bandwidth crossover when given arbitrary Mueller data.

5.1 Filtering

Typically crosstalk can be "mitigated" by using filters around the channels to suppress or apodize the region where crosstalk occurs. This does not fully mitigate the corruption from crosstalk however because

- Filters which apodize in some way result in smoothing of the data, essentially removing information.
- Similar to the above, apodization or cutoff from the filters essentially reduces the bandwidth of the resulting Mueller data.
- Filters won't help much in the case where a great deal of crosstalk is present.

Filtering is needed, but cannot fully alleviate the crosstalk issue. Filtering will not be addressed in depth here; the literature on filtering is vast and mature in control theory and electrical engineering. Keep in mind, however, that if the statistics of the objects being measured are known, then optimal filters can be designed.[26]

6. MAXIMIZING BANDWIDTH

Our focus will be on increasing relative bandwidth to reduce crosstalk, and subsequently increasing the system resolution or speed for spatio-temporally modulated active polarimetric systems. In order to maximize the relative bandwidth, we must think about the system in a way which addresses *efficiency*, otherwise an optimizer will increase the maximum frequency (and hence the relative frequency distance between channels) *ad infinitum* until a specification is met. We also don't have instruments with arbitrary measurement bandwidth. In order to constrain the bandwidth maximization to relative frequencies, we can normalize all of the channels to be contained in a cube (or rectangular prism in certain cases) where the maximum frequency is normalized to be some fixed value. We can choose different norms to accomplish this as long as we are consistent. The two simplest methods are 1) normalize in a 2-norm way, that is your maximum frequency is taken as a vector and normalized by its 2-norm length, and all other channels are also normalized by this same length, or 2) normalize in an ∞-norm way, that is normalize each frequency domain coordinate by the respective maximum frequency

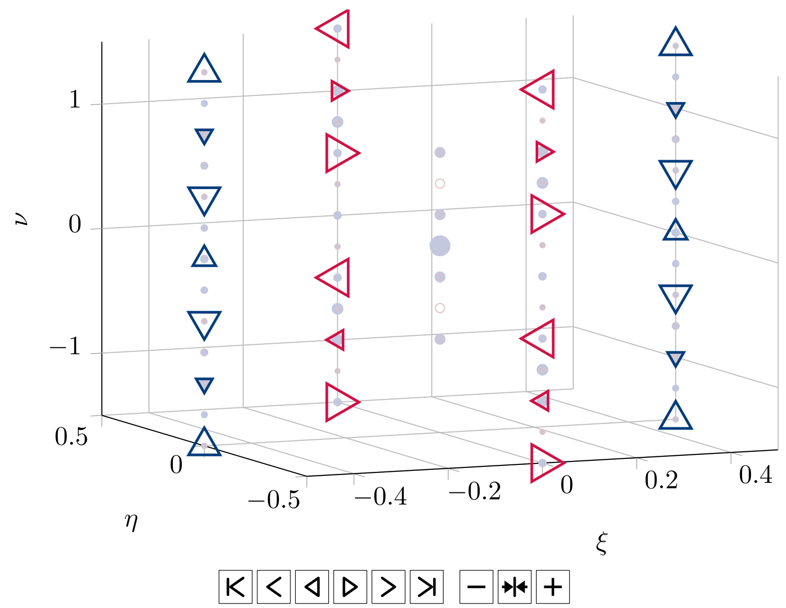

Figure 4: An example of varying frequency parameters to move channels around in the channel space. Note the cancellation/addition at certain parameter values which opens up more bandwidth between the channels. Animated in the electronic version, use the controls displayed to view.

channel domain coordinate. This is what we do for our system examples here. To clarify with an example, suppose that our maximum frequency channel is located at $[0.5, 0.5, 60]^T$, then the normalization factors would be

$$n_{2\text{-norm}} = \sqrt{0.5^2 + 0.5^2 + 60^2} \tag{24}$$

$$n_{\infty\text{-norm},0} = 0.5 \tag{25}$$
$$n_{\infty\text{-norm},1} = 0.5 \tag{26}$$
$$n_{\infty\text{-norm},2} = 60 \tag{27}$$
$$\tag{28}$$

and for an arbitrary channel located at $\boldsymbol{c}_{\text{arb}} = \begin{bmatrix}\xi_{\text{arb}} & \eta_{\text{arb}} & \nu_{\text{arb}}\end{bmatrix}^T$ the two normalizations would be

$$\boldsymbol{c}_{\text{arb},2\text{-norm}} = \frac{\boldsymbol{c}_{\text{arb}}}{\sqrt{0.5^2 + 0.5^2 + 60^2}} \quad \text{and} \quad \boldsymbol{c}_{\text{arb},\infty\text{-norm}} = \begin{bmatrix} \frac{\boldsymbol{\xi}_{\text{arb}}}{0.5} \\ \frac{\boldsymbol{\eta}_{\text{arb}}}{0.5} \\ \frac{\boldsymbol{\nu}_{\text{arb}}}{60} \end{bmatrix} \tag{29}$$

In the examples here, we only normalize the locations of frequency corresponding to the temporal domain, ν, because the examples assume a fixed micropolarizer array which cannot be changed.[1] This results in normalization of the spatial frequency coordinates having no effect on the analysis, but in general, if optimization over spatial frequency is an option, the spatial frequency channel coordinates would also need to be normalized. Normalization ensures that for a relative bandwidth optimization we are making an *oranges to oranges* comparison as channel location changes. Note that the use of different normalization types will lead to different optimization outcomes.

6.1 Channel cancellation

The next step is to attempt to maximize the relative channel bandwidth, now that the channels are all normalized to a maximum frequency. This maximization can typically be accomplished by optimizing over the system channel structure's free parameters $\boldsymbol{p}$ as described in Eqn. 17. Typical parameters for a spatio-temporally modulated polarimeter (which is not spectrally modulated) include

- retardance and retarders, spatially or temporally modulated.
- spatial or temporal analyzer/diattenuator modulation.
- rotation or rotators; these elements are typically combined with one of the types listed above to achieve a modulation.

For a separable channel structure, only channel cancellation/combination or reduction of overall channels may be used to increase the relative bandwidth. Fig. 4 shows channel combination as relative retarder frequency is changed for a quad-retarder + micropolarizer array system. At certain relative frequencies, channels combine or cancel depending on their magnitudes, providing larger distance (bandwidth) between channels. Running an optimizer over a cost function can then find an optimal channel structure, given your free parameters $\boldsymbol{p}$. An example of an optimal (to the best of our knowledge) channel structure for the quad retarder + micropolarizer array system is shown in Fig.5.

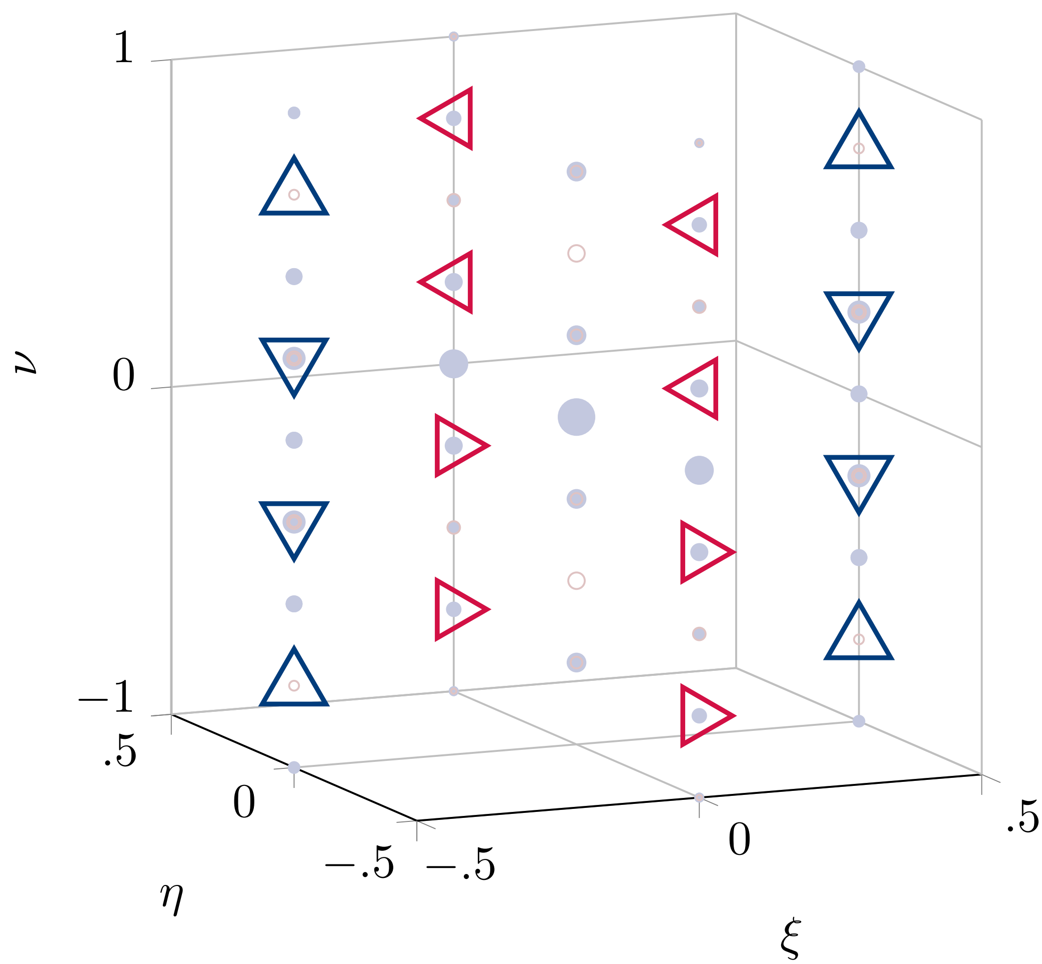

Figure 5: Optimal channel structure for a specific quad retarder + micropolarizer channel structure for m_{23}. Reproduced from a figure in Vaughn *et al.*[1]

6.2 Discussion

Once the channeled system framework is understood, and the free parameters, $\boldsymbol{p}$ of a spatio-temporally modulated system are specified or known, then it is straightforward to design a cost function and run an optimizer over that function to optimize for bandwidth or jointly for bandwidth, noise, and other constraints. The most difficult part of directly optimizing in the channel space is not, however, defining a cost function and running an optimization against the cost function. The difficult task is designing a model which properly describes the channel structure itself, with proper physical constraints. We have designed a model for the specific case of a quad-retarder + micropolarizer array system, but we hope to adapt our current model to generate generic spatio-temporally modulated systems in the near future.

Additionally, if the statistics of an object or set of objects are known, then non-uniform bandwidth can be maximized. All of the examples shown in this communication optimize for an equal channel bandwidth between all channels. In certain cases, more bandwidth may be wanted for certain sets of channels over other sets of channels and for certain Mueller matrix elements. This can all be accomplished by using the appropriate cost function, but is non-trivial due to the channel mixing which occurs between Mueller matrix elements.

7. NOISE AND SYTEMATIC ERROR

The channel bandwidth optimization discussed in the previous section must be paired with the sensitivity of the system to deviations from the ideal optimized parameters, i.e., an actual system will have non-ideal modulations and modulator elements. We present some preliminary results on systematic deviations here, but we have not fully worked out how to measure the sensitivity of a system's channel structure to systematic deviations (often called systematic error in the literature). The sensitivity to random noise sources is also discussed here, but again we have not worked out a general systematic way to compute the sensitivity of channel structures to random noise when bandwidth is taken into account (including filtering effects). Noise effects from the inversion of the $\boldsymbol{Q}$ matrix, however, have been addressed.[2]

7.1 Systematic error

Systematic error will occur when the actual system deviates from the designed system, or when there is some consistent bias due to physical instrument details. Here systematic error for a channeled system refers to the differences between the real system's channels as compared with the ideal channels from some designed channel structure. Issues arise for a separable channeled system when channel cancellation/combination has been used as a tool to increase system bandwidth.

For separable channeled systems a potentially serious problem arises: at the locations in the frequency space where the channel cancellation(s) occurred, channels will again be present due to deviations of real components. These *spurious channels* will be convolved with Mueller data, and introduce channel crosstalk. We really only have one option available, to minimize the magnitude of these spurious channels so that the crosstalk into the adjacent channels is low. An example of is shown in Fig. 6, the small triangles represent the spurious channels.

We have found a way to reduce the effects of the spurious channels for the quad retarder + micropolarizer system, which was to re-optimize over our channels using the remaining free parameters available while fixing the ones constrained by the physical instrument components. In our quad-retarder + micropolarizer system example, once our actual retardances were fixed, we re-optimized using the starting position of each retarder and added a parameter to our cost function which characterized the magnitudes of the spurious channels compared with the magnitudes of the adjacent channels. For general spatio-temporal systems this kind of method will work after some of the physical components are specified, if there are any free parameters left to optimize over.

In fact, an iterative approach would likely yield the best results with a single component at a time being sourced, measured and characterized, then the system can be re-optimized to reset the other components specifications to minimize the crosstalk, and then the process is repeated.[27]

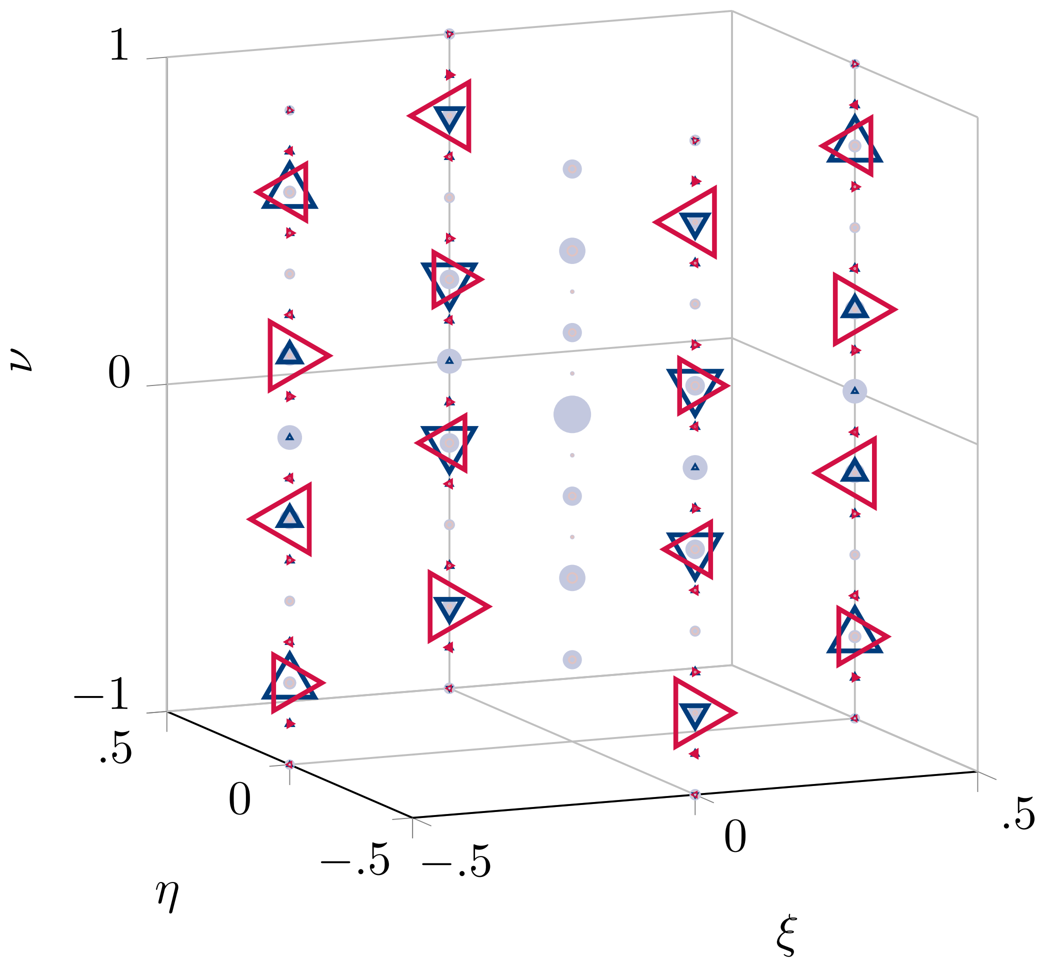

Figure 6: An example of systematic error in a real instrument, the small triangles represent channels which are present due to retardance deviation from the specifications.

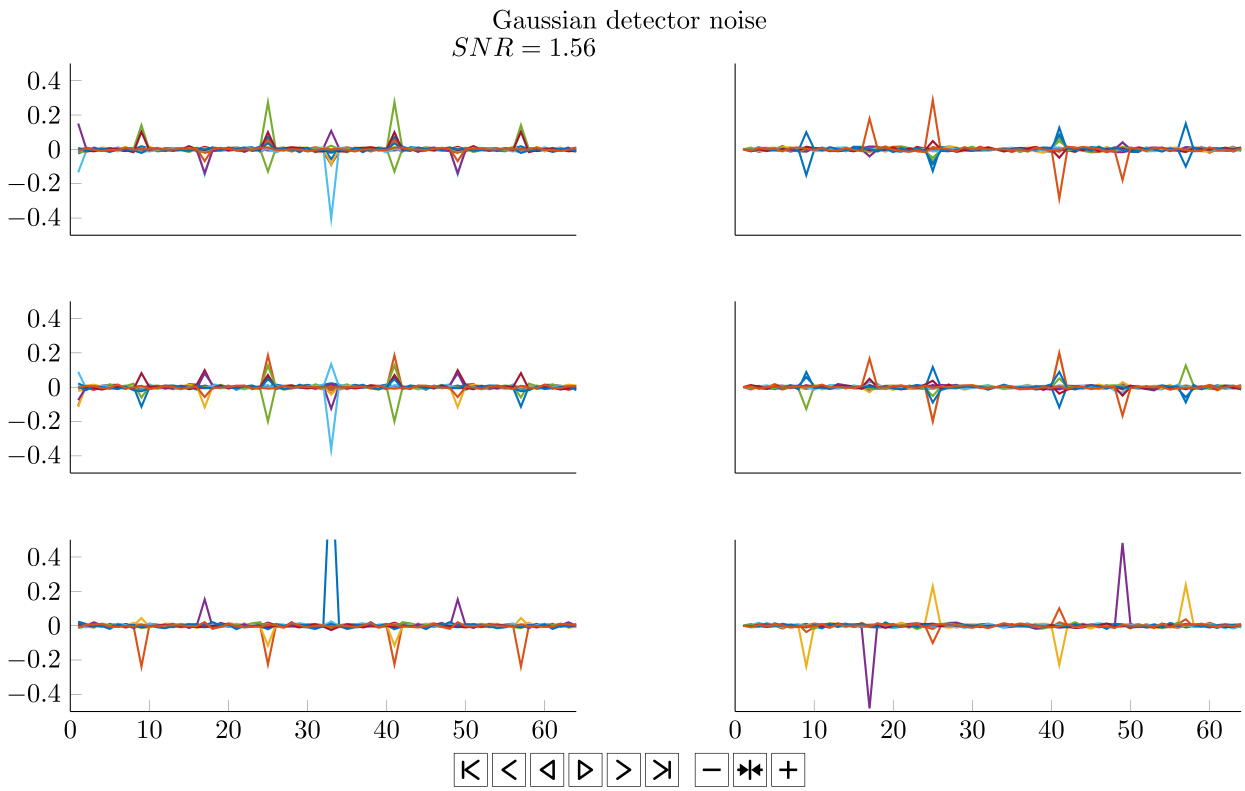

Figure 7: Gaussian detector noise effects on channel structure. Note that these are the same channels as shown in Fig. 6, but plotted along the ν lines. The left column is the real part, the right column is the imaginary part, there are 16 colors in each graph representing each Mueller matrix element. The first row is ν at $\xi = 0, \eta = -0.5$, the second row is ν at $\xi = -0.5, \eta = 0$ and the third row is ν at $\xi = 0, \eta = 0$. Animated in the electronic version.

7.2 Noise

The other impacts to real channeled systems are random noise, for instance detector noise. The results presented here are preliminary, and we only modeled detector Johnson (Gaussian like) noise for the detector. The results are simulated, but show that the channel structure itself is quite robust to detector noise. Here we switch to a different view of the channels to better view the noise effects. Each line of channels in the ν direction is plotted in Fig. 7 and Gaussian noise is added in a simulation to the final irradiance for this result. The SNR is shown in the figure, and it appears that the channel structure is stable for an SNR above somewhere between 1 and 2. This result will need to be validated on the real instrument, and we plan on testing this in the near future.

We have not modeled the effects of noise on the reconstruction for our specific system yet, but noise effects have been addressed for channeled systems by others.[2,22,28]

8. CONCLUSION

Channeled polarimeter design has changed the way that instrument designers approach the design process, and allows engineers to systematically design both general and task specific polarimeters. We have presented examples and some general insight into using channeled system design for spatio-temporally modulated Mueller matrix polarimeters. We also address some of the intricacies of channeled design, and give some preliminary examples of possible systematic errors and noise effects on channel structures. Furthermore, we give an example of how to mitigate some of the systematic errors, and in the future will use a different approach when building a real instrument by re-optimizing the channel structure after each instrument component is sourced. In the future we hope to build a fully generic channeled system model for spatio-temporally modulated instruments, so that the community can design their own instruments in a systematic way. We also need to validate our systematic error mitigation on our real instrument, and validate the effects of noise on the channel structure of a real instrument.

ACKNOWLEDGMENTS

The authors would like to thank Andrey Alenin for his discussions about bandwidth in channeled systems.

This work was supported by the Air Force Office of Scientific Research under award FA-9550-10-0114, the National Science Foundation under award DGE-0841234, and the University of Arizona TRIF Imaging Fellowship Program.

REFERENCES

[1] Vaughn, I. J., Rodríguez-Herrera, O. G., Xu, M., and Tyo, J. S., "A portable imaging mueller matrix polarimeter based on a spatio-temporal modulation approach: theory and implementation," *Proc. SPIE* **9613** (2015).

[2] Alenin, A. S. and Tyo, J. S., "Generalized channeled polarimetry," *J. Opt. Soc. Am. A* **31**, 1013–1022 (May 2014).

[3] Azzam, R. M. A., "Photopolarimetric measurement of the mueller matrix by fourier analysis of a single detected signal," *Opt. Lett.* **2**, 148–150 (Jun 1978).

[4] Oka, K. and Kato, T., "Spectroscopic polarimetry with a channeled spectrum," *Optics Letters* **24**(21), 1475–1477 (1999).

[5] Oka, K., "Singleshot spectroscopic polarimetry using channeled spectrum," in [*Photonics Asia 2002*], 167–175, International Society for Optics and Photonics (2002).

[6] Oka, K. and Kaneko, T., "Compact complete imaging polarimeter using birefringent wedge prisms," *Optics express* **11**(13), 1510–1519 (2003).

[7] Sabatke, D., Locke, A., Dereniak, E. L., Descour, M., Garcia, J., Hamilton, T., and McMillan, R. W., "Snapshot imaging spectropolarimeter," *Optical engineering* **41**(5), 1048–1054 (2002).

[8] Hagen, N. and Dereniak, E. L., "Snapshot mueller matrix spectropolarimetry," in [*Optical Engineering+ Applications*], 668207–668207, International Society for Optics and Photonics (2007).

[9] Kudenov, M. W., Escuti, M. J., Dereniak, E. L., and Oka, K., "White-light channeled imaging polarimeter using broadband polarization gratings," *Applied optics* **50**(15), 2283–2293 (2011).

[10] Hagen, N. and Kudenov, M. W., "Review of snapshot spectral imaging technologies," *Optical Engineering* **52**(9), 090901–090901 (2013).

[11] Dubreuil, M., Rivet, S., Le Jeune, B., and Cariou, J., "Snapshot mueller matrix polarimeter by wavelength polarization coding," *Optics express* **15**(21), 13660–13668 (2007).

[12] LaCasse, C. F., Chipman, R. A., and Tyo, J. S., "Band limited data reconstruction in modulated polarimeters," *Opt. Express* **19**, 14976–14989 (Aug 2011).

[13] LaCasse, C. F., Tyo, J. S., and Chipman, R. A., "Role of the null space of the drm in the performance of modulated polarimeters," *Optics letters* **37**(6), 1097–1099 (2012).

[14] LeMaster, D. A. and Hirakawa, K., "Improved microgrid arrangement for integrated imaging polarimeters," *Opt. Lett.* **39**, 1811–1814 (Apr 2014).

[15] LaCasse, C. F., Ririe, T., Chipman, R. A., and Tyo, J. S., "Spatio-temporal modulated polarimetry," *Proc. SPIE* **8160**, 81600K–81600K–11 (2011).

[16] Myhre, G., Hsu, W.-L., Peinado, A., LaCasse, C., Brock, N., Chipman, R. A., and Pau, S., "Liquid crystal polymer full-stokes division of focal plane polarimeter," *Opt. Express* **20**, 27393–27409 (Dec 2012).

[17] Zhao, X., Bermak, A., Boussaid, F., and Chigrinov, V. G., "Liquid-crystal micropolarimeter array for full stokes polarization imaging in visible spectrum," *Optics express* **18**(17), 17776–17787 (2010).

[18] Wolf, E., [*Introduction to the Theory of Coherence and the Polarization of Light*], Cambridge University Press, New York, United States (2007).

[19] Collett, E., "Polarized light. fundamentals and applications. 1993."

[20] Gil, J. J., "Characteristic properties of mueller matrices," *Journal of the Optical Society of America A* **17**, 328–334 (2000).

[21] Chipman, R., "Handbook of optics: Volume i: Geometrical and physical optics, polarized light, components and instruments," (2009).

[22] Alenin, A. S. and Tyo, J. S., "Task-specific snapshot mueller matrix channeled spectropolarimeter optimization," (2012).

[23] Nyquist, H., "Certain topics in telegraph transmission theory," *American Institute of Electrical Engineers, Transactions of the* **47**(2), 617–644 (1928).

[24] Gabor, D., "Theory of communication. part 1: The analysis of information," *Journal of the Institution of Electrical Engineers-Part III: Radio and Communication Engineering* **93**(26), 429–441 (1946).

[25] Shannon, C. E., "A mathematical theory of communication," *ACM SIGMOBILE Mobile Computing and Communications Review* **5**(1), 3–55 (2001).

[26] LaCasse, C. and Tyo, S., "Modulated polarimeter operators in the presence of stochastic signals," in [*SPIE Defense, Security, and Sensing*], 836403–836403, International Society for Optics and Photonics (2012).

[27] Snik, F., Harten, G. v., Alenin, A. S., Vaughn, I. J., and Tyo, J. S., "A multi-domain full-stokes polarization modulator that is efficient for 300-2500nm spectropolarimetry," *Proc. SPIE* **9613** (2015).

[28] Sabatke, D., Descour, M., Dereniak, E., Sweatt, W., Kemme, S., and Phipps, G., "Optimization of retardance for a complete stokes polarimeter," *Optics Letters* **25**(11), 802–804 (2000).